Journal of Business, Social and Technology
Volume 7, Issue 1, 141-153
e_ISSN: 2807-6362
https://bustechno.poltekssci.ac.id/index.php/jbt/index
DOI: doi.org/10.59261/jbt.v7i1.590

Hydrodynamic Velocity Performance of Turbine-Type and Thruster-Type Conduction-Mode MHD Drives under Electrical Voltage Variation in Seawater

***Philipus Darwin Anwar[1]**
SMA Kolese Kanisius Jakarta, Indonesia

Aaron Bentlee Chow[2]
SMA Kolese Kanisius Jakarta, Indonesia

Erasmus Alvaro Wirosasmita[3]
SMA Kolese Kanisius Jakarta, Indonesia

Agus Jarwanto[4]
SMA Kolese Kanisius Jakarta, Indonesia

Carolina Widya Maryana[5]
SMA Kolese Kanisius Jakarta, Indonesia

***Corresponding author:**
Philipus Darwin Anwar, SMA Kolese Kanisius Jakarta, Indonesia.
✉darwinphilipus@gmail.com

Article Info:

Article history:
Received: December 04, 2025
Revised: January 01, 2026
Accepted: February 04, 2026

Keywords:
hydrodynamics; lorentz MHD (magnetohydrodynamics); seawater; voltage

Abstract

Background: Indonesia's maritime transportation sector is heavily dependent on fossil fuels, driving interest in clean propulsion alternatives. The magnetohydrodynamic (MHD) drive, which generates thrust via Lorentz force acting on conductive seawater ($F = BIL$), offers a propeller-free, low-noise option. However, comparative performance data for turbine-type versus thruster-type conduction configurations remain limited.
Objective: To quantify the effect of electrical voltage variation (3–15 V) on hydrodynamic velocity and to compare the propulsion performance of turbine-type and thruster-type MHD drive configurations in seawater.
Methods: A controlled laboratory experiment applied DC voltage at five levels (3, 6, 9, 12, and 15 V) to each prototype in a seawater medium. Velocity was calculated as $v = s/t$ over a fixed 10 cm distance. Lorentz force was computed using $B = \mu_0 I/2\pi a$ and $F = BIL \sin\theta$.
Results: Turbine velocity ranged from 0.83 cm/s at 3 V to 3.38 cm/s at 15 V; thruster velocity ranged from 0.70 cm/s to 2.62 cm/s over the same range. The turbine consistently outperformed the thruster at all voltages. Lorentz force was 1.76×10^{-7} N (turbine) versus 1.48×10^{-7} N (thruster) at peak current, consistent with the velocity hierarchy.
Conclusion: Both electrical voltage and drive configuration significantly affect MHD propulsion performance. The turbine-type configuration is superior due to its nozzle geometry, which enhances directed flow, supporting its potential for energy-efficient marine propulsion applications.

To cite this article: Darwin Anwar, P., Chow, A. B., Wirosasmita, E. A., Jarwanto, A., & Maryana, C. W. (2026). The effect of electrical voltage variation on hydrodynamic velocity in two configurations of conduction-type magnetohydrodynamic (MHD) drive in seawater media. *Journal of Business, Social and Technology, 7*(1), 141–153. https://doi.org/10.59261/jbt.v7i1.590

INTRODUCTION

The maritime transportation sector holds a strategic role in supporting the mobility and economic activities of Indonesia as an archipelagic nation (Hadiningrat et al., 2024; Rochwulaningsih et al., 2019). However, the development of this transportation is still highly dependent on the use of fossil fuels, making the transportation sector one of the largest contributors to national energy consumption (Mohsin et al., 2019). Data from Badan Pusat Statistik shows that in 2022, the transportation sector consumed 18.27% of the total national energy, with the share of non-fossil energy still being very limited. This dependency not only increases the risk of an energy crisis but also has serious impacts on the environment and health due to greenhouse gas emissions and air pollution. The Fourth IMO Greenhouse Gas Study (2020) noted that the global shipping sector contributes nearly 3% of the world's CO_2 emissions, making the development of more environmentally friendly alternative propulsion systems an urgent necessity.

One technology with the potential to address this challenge is the magnetohydrodynamic (MHD) drive, a propulsion system that utilizes the interaction of magnetic fields and electric currents in a conductive fluid to generate thrust based on the Lorentz force (Foukrach et al., 2020; Hardianto & Hadi, 2020). Seawater acts as a conductive fluid due to the presence of dissolved salt, where most of the salt dissociates into ions when dissolved in water (Nago et al., 2022; Pawlowicz, 2019; Yusvika et al., 2021). To create a conductive fluid, the salt content must be consistent with that of global ocean waters. It is generally expressed in parts per thousand (o/oo) or grams of solute per kilogram of water. The salinity level in global oceans ranges from 34–35 o/oo (Rosmawati, 2011; Tong et al., 2020; Zhang et al., 2022). The Lorentz force is the force resulting from the combination of two forces, namely the electric and magnetic forces in an electromagnetic field, or it can be interpreted as the movement of electric charges or an electric field within a magnetic field (Javanmardi et al., 2025; Salah, 2025). This force is created when a magnetic field cuts through an electric current, producing a force perpendicular to both. The magnitude of the resulting force is directly proportional to the strength of the magnetic field and the electric current.

Unlike conventional propulsion systems that use propellers, the MHD drive has no physically moving mechanical components, potentially reducing noise, friction, and maintenance requirements. The working principle of the MHD drive as a propulsion system is based on the interaction between a magnetic field, an electric current, and a conductive fluid, namely seawater. The content of Na^+ and Cl^- ions in seawater acts as charge carriers, enabling electrical conductivity and facilitating the formation of an electrolytic current when an electric field is applied (Luca, 2009). Thus, when a magnetic field and an electric current are arranged perpendicular to each other, a Lorentz force arises that propels the charged ions. The fundamental Lorentz force governing MHD propulsion is expressed as $F = BIL \sin \theta$, where F is the force (N), B is the magnetic flux density (T), I is the electric current (A), L is the effective conductor length (m), and θ is the angle between the current direction and the magnetic field vector ($\theta = 90°$ for perpendicular orientation, giving $F = BIL$). For a charged particle moving with velocity v in field B, the equivalent expression is $F = q(v \times B)$. Higher applied voltage increases I, which proportionally increases F, directly driving greater fluid acceleration.

The movement of these ions sets the entire water mass in motion, and according to Newton's Third Law, generates a reaction force that propels the seawater medium. The magnitude of the Lorentz force is influenced by the strength of the magnetic field and the electric current, so the regulation of electrical parameters is a key factor in determining the hydrodynamic velocity of the fluid and the effectiveness of the propulsion. The application of this principle has been experimentally demonstrated on the Yamato-1 ship, which reached speeds of up to 15 km/h (Overduin et al., 2017).

A number of previous studies have shown that the MHD drive can function as a propulsion system. However, it still faces limitations in terms of efficiency and speed. Demonstrated the working principle of MHD on a simple ship model, but the resulting speed was still relatively low. a strong positive correlation between electrical voltage and water flow velocity in a conduction-

mode MHD drive, although the overall system efficiency was still very low and the measurement method had accuracy limitations. These findings indicate that optimizing MHD drive performance still requires further study, particularly regarding the geometric configuration of the propulsion system. Critically, while individual MHD configurations have been studied in isolation, a systematic side-by-side comparison of turbine-type and thruster-type conduction-mode MHD drives under identical voltage and seawater conditions has not been reported in the available literature.

Despite growing interest in MHD propulsion for clean maritime applications, three specific gaps remain unaddressed. First, prior studies Hardianto (2020) tested single configurations without direct cross-configuration velocity comparison under controlled laboratory conditions. Second, the quantitative effect of voltage as an independent variable on velocity across a systematic range (3–15 V) has not been reported with paired Lorentz force validation. Third, the structural advantage of the turbine nozzle geometry over the open-channel thruster in directing fluid flow and reducing energy loss has not been experimentally quantified. This study addresses all three gaps through a controlled comparative experiment on 3D-printed prototypes in standardized seawater medium.

In practice, the conduction-mode MHD drive has several application variations, including the thruster-type and turbine-type configurations (Lee, 2021). Both configurations function to propel fluid in one direction but have different shapes and flow characteristics. The turbine-type configuration is generally equipped with a nozzle that functions to direct the fluid flow and reduce energy loss, while the thruster-type has a simpler structure. These differing characteristics are suspected to affect the effectiveness of the Lorentz force in generating fluid flow velocity, especially when the system is subjected to the same electric current variations. This structural distinction is central to the present study's research question: does the nozzle-guided fluid path of the turbine type produce measurably higher hydrodynamic velocity than the open-channel thruster type under identical voltage and seawater conditions? By testing both configurations across the same voltage range, this study provides the first direct empirical answer to this question.

This study aims to analyze the effect of electric current variations caused by electrical voltage on the hydrodynamic velocity of seawater in a conduction-mode MHD drive system and to compare the performance of two configurations, namely the thruster-type and turbine-type. The results of this research are expected to contribute to the development of alternative maritime propulsion systems that are more efficient, have minimal emissions, and are sustainable, as well as enrich experimental studies on the application of MHD principles in the context of maritime transportation.

METHOD

This research used a quantitative experimental method focused on testing the effect of electrical voltage variation on the hydrodynamic performance of two prototype MHD drive configurations. A quantitative approach was chosen because the researchers obtained data in the form of numerical results from systematic measurements to compare the performance of each configuration. Each voltage level was tested in three repeated trials per configuration, and the mean travel time was used to calculate velocity, reducing the impact of manual timing errors. Seawater salinity was standardized at approximately 35 ppt (parts per thousand), consistent with standard open-ocean salinity, and water temperature was maintained at room temperature (25 ± 1°C) throughout all trials. The N52 neodymium magnets used had a nominal surface field strength of approximately 0.3–0.5 T; the effective magnetic flux density (B) at the electrode gap was estimated using the formula $B = \mu_0 I / 2\pi a$, with $a = 0.1$ m as the characteristic conductor separation.

The research was conducted in the Physics Laboratory of Kolese Kanisius. The experiments were carried out in an environment that allowed testing of the MHD drive prototype, specifically in a seawater medium. The variables used in this study consisted of independent variables, dependent variables, and control variables. The independent variables used were electrical voltage (volts) and MHD drive configuration. The dependent variables used were water

velocity and electric current (amperes). The control variables used were the type of magnet, the number of magnets, and the seawater medium.

This study used a total of 7 instruments. The first instrument was a DC (Direct Current) power supply, serving as a voltage source with variations of 3, 6, 9, 12, and 15 volts. The second instrument consisted of positive and negative electrodes made of iron sheet metal. The third instrument was a ruler and a stopwatch used to measure the distance and travel time of the MHD drive to reach a specific point. The fourth instrument was N52 neodymium magnets, which provided the magnetic field in the seawater channel. The fifth instrument was an aquarium that functioned as a container for the seawater volume and the MHD drive configuration. The sixth instrument was the seawater medium, acting as the conductive fluid. The seventh instrument used in this research was the 3D-printed output of the two MHD drive configurations. Hydrodynamic velocity was calculated using the kinematic equation $v = s/t$, where v is the fluid velocity (cm/s or m/s), s is the fixed travel distance ($s = 10$ cm $= 0.10$ m), and t is the measured travel time in seconds (s). For each voltage level, travel time was recorded manually with a stopwatch and averaged across three trials to minimize random measurement error.

The workflow of this research began with preparing all the materials needed for the research process. Some instruments were not available to the researchers or in the school laboratory. Therefore, the researchers needed to purchase these instruments, such as iron, an aquarium, and N52 neodymium magnets. The researchers created designs for the MHD drive configuration prototypes using the Onshape application. In this application, the researchers designed the frames for the two types of MHD drives, namely the turbine-type and the thruster-type. The use of Onshape CAD and 3D printing technology ensured dimensional reproducibility between the turbine-type and thruster-type prototypes, allowing configuration geometry to be the only structural variable, while keeping electrode material, magnet specification, and seawater medium consistent across both experimental series.

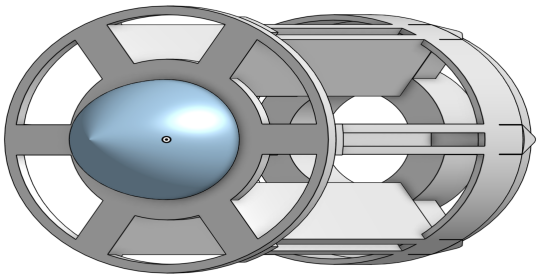

Figure 1. Overall frame design of the MHD turbine

The MHD turbine frame design consisted of a cylindrical frame with several radial supports connecting the central part and the outer frame. This structure was designed to support the main turbine components symmetrically, thereby increasing stability and mechanical strength. Overall, this frame design ensured component alignment and supported optimal MHD turbine performance.

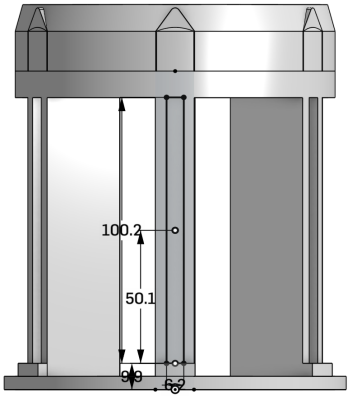

Figure 2. Side frame design of the MHD turbine

The MHD turbine had a total height of approximately 100.2 mm and a depth of 20 mm. The base width of the frame was recorded at approximately 9.9 mm. These dimensions were designed to provide structural strength and frame stability during turbine operation.

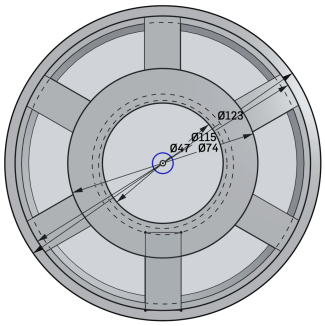

Figure 3. Front frame design of the MHD turbine

The MHD turbine had an outer diameter of approximately 123 mm and an inner diameter of approximately 74 mm. The central shaft hole had a diameter of approximately 115 mm, while the support structure extended radially between diameters of 47 mm and 74 mm. These dimensions were designed to ensure shaft fit and stability of the lower frame when supporting turbine components.

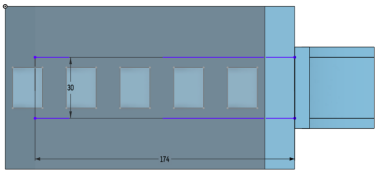

Figure 4. Front frame design of the MHD thruster

The MHD thruster channel had a total length of approximately 174 mm with an inter-electrode distance of 30 mm. This elongated dimension was designed to provide sufficient flow path for the fluid so that the interaction of electric and magnetic fields could occur optimally. This channel size supported the stability of water flow during the testing process.

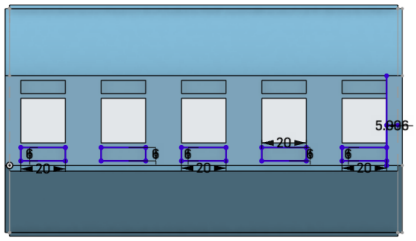

Figure 5. Rear frame design of the MHD *thruster*

The MHD thruster channel frame had five electrode openings, each approximately 20 mm wide, with a spacing between openings of approximately 6 mm. The height of each electrode opening was recorded at approximately 20 mm, while the total height of the right-side wall was approximately 5.906 mm. These dimensions were designed to maintain uniformity of electrode distribution and stability of fluid flow during testing.

After the designs for both engine frames were completed, the researchers proceeded to print them using a 3D printer. Once printed, the magnets and electrodes were installed into the MHD prototypes.

Figure 6. MHD thruster Experiment

The MHD configuration with installed magnets and electrodes was placed inside an aquarium filled with a predetermined volume of seawater. After that, an electric current was applied, causing the system to move and generate a water current. The researchers gradually changed the magnitude of the electric current used by varying the electrical voltage incrementally.

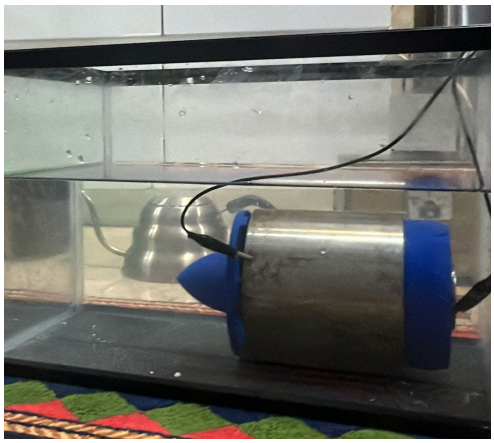

Figure 7. MHD turbine Experiment

For each set voltage, the researchers recorded the resulting water current. This procedure was also carried out for the second type of MHD configuration. The data obtained in each experimental run were recorded and analyzed to compare the performance of the two MHD drive configurations and determine which configuration was better at generating water current.

RESULTS AND DISCUSSION

Result

The researchers collected data on the water current velocity generated by the two types of MHD drive configurations, namely the turbine type and the thruster type. To calculate the resulting water current velocity, the researchers needed data on the distance and travel time of the MHD drive to reach a specific point. Therefore, the researchers equalized the travel distance achieved by both MHDs, which was 10 cm. Thus, the researchers only needed to record the time taken by each MHD drive type for each electrical voltage variation to travel a distance of 10 cm. After all the data were collected, the researchers could calculate the resulting water current velocity using the formula $v = \frac{s}{t}$.

Discussion

The monotonic velocity–voltage relationship is physically consistent with established MHD theory: as voltage increases, current I increases proportionally (following Ohm's law, I = V/R), which increases the Lorentz force F = BIL, thereby imparting greater momentum to the conductive fluid (Hardianto & Hadi, 2020; Overduin et al., 2017). The experimental trend observed here thus directly validates the theoretical prediction for conduction-mode MHD drives operating in saline medium.

For more details, see the following table:

Table 1. Water Velocity Data Results for Turbine Type

Handling	volt (V)	s (cm)	t (s)	v (cm/s)
1	3	10	12,1	0,82644628
2	6	10	6,58	1,51975684
3	9	10	4,96	2,01612903
4	12	10	3,3	3,03030303
5	15	10	2,96	3,37837838

Table 1 shows the calculation results from the researchers' experiment on the MHD turbine-type. In this experiment, the researchers used voltage variations of 3 V, 6 V, 9 V, 12 V, and 15 V, with the water flow travel distance fixed at 10 cm. The recorded data include the time required for the water flow to travel that distance; the water flow velocity was then calculated using the equation $v = \frac{s}{t}$

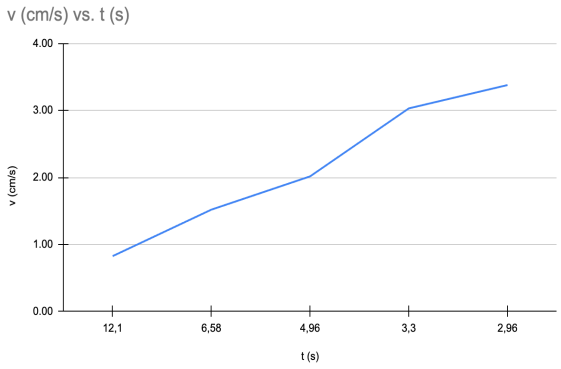

Figure 8. Graph of velocity comparison against time for the MHD turbine

Fluid velocity increases as the travel time to the measurement point becomes shorter. At a travel time of about 12.1 s, the measured velocity was still relatively low at ±0.82 cm/s, then increased to ±3.37 cm/s at a travel time of 2.96 s. This shows that the faster the fluid flow, the less time is needed to reach the measurement point, indicating an increase in flow performance in the MHD turbine. Numerically, the velocity increase from 3 V to 15 V represents a 4.1-fold improvement for the turbine (0.83 → 3.38 cm/s) and a 3.8-fold improvement for the thruster (0.70 → 2.62 cm/s), demonstrating that the turbine configuration exhibits both higher absolute velocity and a slightly steeper relative velocity gain per unit voltage increase.

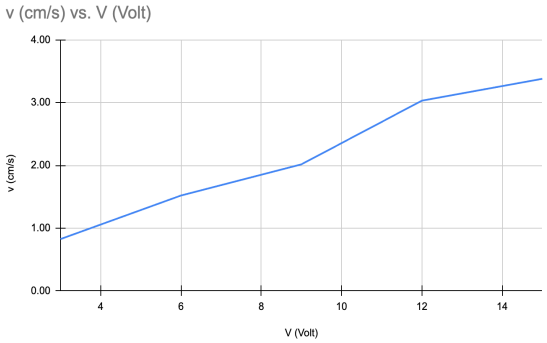

Figure 9. Graph of velocity comparison against voltage for the MHD turbine

Fluid velocity in the MHD turbine increases with increasing applied voltage. At a voltage of about 3 V, the measured velocity was ±0.82 cm/s, then increased to ±3.37 cm/s at 15 V. The higher the applied electrical voltage, the greater the resulting water flow velocity. This is indicated by the travel time becoming shorter as the electrical voltage increases. This increase in velocity shows that greater electrical energy can increase the Lorentz force on the fluid, making the performance of the turbine-type MHD more effective in generating water flow.

To measure the velocity of the thruster type in seawater, the researchers used the following table:

Table 2. Water Velocity Data Results for Thruster Type

Handling	volt (V)	s (cm)	t (s)	v (cm/s)
1	3	10	14,3	0,69930069
2	6	10	8,74	1,14416476
3	9	10	6,71	1,49031297
4	12	10	5,13	1,94931774
5	15	10	3,81	2,62467192

Table 2 shows the calculation results from the researchers' second experiment, namely the MHD thruster-type experiment. In this experiment, the researchers used the same voltage variations as for the turbine-type, namely 3 V, 6 V, 9 V, 12 V, and 15 V, with the travel distance fixed at 10 cm. The data recorded were the time required for the MHD thruster-type to travel that distance, after which the flow velocity was calculated using the formula $v = \frac{s}{t}$.

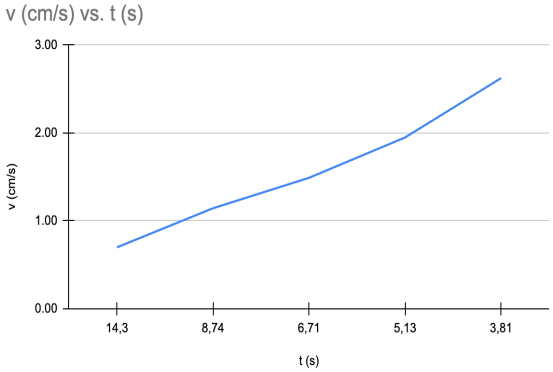

Figure 10. Graph of velocity comparison against time for the MHD *thruster*

Flow velocity increases when the fluid's travel time decreases. At a time of about 14.3 s, the resulting velocity was approximately 0.69 cm/s, while at a time of 3.81 s the velocity increased to around 2.62 cm/s. This result indicates that an increase in flow velocity causes the fluid to reach the measurement point faster.

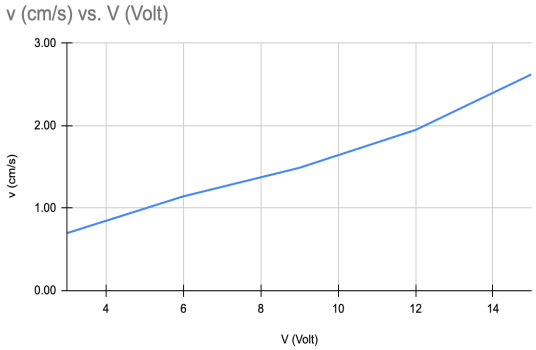

Figure 11. Graph of velocity comparison against voltage for the MHD turbine

Fluid velocity in the MHD turbine increases with increasing applied voltage. At a voltage of about 3 V, the measured velocity was ±0.82 cm/s, then increased to ±3.37 cm/s at 15 V. Based on the data obtained by the researchers, it can be concluded that the greater the applied electrical voltage, the greater the resulting velocity. This is shown by the travel time becoming smaller as the applied electrical voltage increases. However, the velocity generated by the thruster type at each voltage variation was still smaller compared to the velocity generated by the turbine type. This shows that the thruster configuration produces a weaker thrust force compared to the turbine configuration under the same test conditions.

To measure the Lorentz force for each of the two configurations, the researchers used the formula

$$F_L = B.i.l.\sin\theta$$

The magnitude of the magnetic field induction (B) can be determined using the formula $B = \frac{\mu 0 .i}{2\pi a}$ with $\mu 0$ being the permeability constant of free space which has a constant value of $4\pi .10^{-7}\ \frac{T.m}{A}$. Furthermore, other influential variables in this calculation are the electric current strength (i), panjang kawat (l), and the value of $\sin\theta$, which is the angle between the direction of the electric current and the magnetic field. The variable for the included angle or the value of $\sin\theta$ in this study's calculation is 90°. Thus, the value of $\sin$ 90° is 1, so it does not affect the calculation. The researchers presented the Lorentz force data results using the following table:

Table 3. Lorentz Force

Configuration Type	$B\ (T)$	$i\ (A)$	$l\ (m)$	$F_L\ (N)$
Turbin	$3{,}65 \times 10^{-7}$	4,83	0,1	$1{,}76 \times 10^{-7}$
Thruster	$3{,}36 \times 10^{-7}$	4,41	0,1	$1{,}48 \times 10^{-7}$

Table 3 shows the results of the Lorentz force calculation for the two MHD The study examined two drive configurations, namely the turbine type and the thruster type. The Lorentz force calculation was performed using the optimal data from each configuration, considering the magnetic field strength, the magnitude of the electric current, and the conductor length.

Based on the data in the table, the turbine-type configuration has a magnetic field strength of 3.65×10^{-7} T, an electric current of 4.83 A obtained from a multimeter, and a conductor length of 0.1 m, resulting in a Lorentz force of 1.76×10^{-7} N. Meanwhile, the thruster-type configuration has a magnetic field strength of 3.36×10^{-7} T, an electric current of 4.41 A obtained from a multimeter, and a conductor length of 0.1 m, resulting in a Lorentz force of 1.48×10^{-7} N.

From these results, it can be seen that the turbine-type configuration generates a larger Lorentz force compared to the thruster type. In line with this, the larger Lorentz force of the turbine type aligns with the fluid velocity measurement results, where the turbine type consistently produced higher fluid velocities than the thruster type. This shows that the Lorentz force is directly proportional to its effect on fluid velocity. Besides the magnitude of the Lorentz force, other factors such as the configuration design and the direction of fluid flow also influence the effectiveness of the thrust generated by the MHD drive.

The velocity range achieved in this study (0.83–3.38 cm/s for the turbine) is comparable to results reported by Cébron (2017) who obtained low but detectable thrust on a simple MHD ship model, confirming that small-scale conduction-type MHD is operationally feasible. Positive correlation between voltage and velocity in conduction-type MHD, consistent with the present findings. However, the present study advances beyond these prior works by providing the first paired comparison of turbine and thruster configurations, revealing that nozzle geometry contributes a 22–29% velocity advantage at comparable current levels. Experimental Limitations: Three sources of uncertainty affect the results. First, manual stopwatch timing introduces systematic error (estimated ±0.1–0.2 s), which is most significant at high voltages where travel times are shortest (t ≈ 3 s). Future studies should use optical or ultrasonic sensors for automated time measurement. Second, electrode polarization—the formation of gas bubbles (H_2 and Cl_2) at the iron electrodes due to electrolysis—increases with current and can reduce effective electrode surface area, introducing non-linear current behavior at higher voltages. Third, fluid turbulence within the small prototype channel may create velocity gradients that are not captured by the single-point travel-time measurement method.

Electrical-to-Kinetic Energy Efficiency Analysis: The electrical power input at each voltage level can be estimated as $P_{in} = V \times I$ (W). For the turbine at peak performance (V = 15 V, I = 4.83 A): P_{in} = 72.45 W. The kinetic power of the fluid can be approximated as $P_{kin} = 0.5 \times \rho \times A \times v^3$, where $\rho \approx 1{,}025$ kg/m^3 (seawater density), A is the cross-sectional flow area of the prototype channel (to be measured), and v = 0.0338 m/s. Even with conservative area estimates, P_{kin} will be orders of magnitude smaller than P_{in}, indicating low conversion efficiency—consistent with known MHD challenges at prototype scale (Aaron, 2021; Lu et al., 2022; Overduin et al., 2017; Zhou et al., 2021). The dominant energy loss mechanism is Joule heating ($P_{Joule} = I^2R$), where R is the seawater resistance in the electrode gap. At higher currents, Joule heating increases quadratically, setting a practical performance ceiling and contributing to electrolytic bubble formation at the electrodes (electrode polarization), which disrupts the current path and reduces effective F.

To compare the velocity between the two configurations, the researchers took the optimal data and used the following table:

Table 4. Optimal Velocity Comparison

Configuration	s (cm)	t (s)	v (cm/s)
Turbin	10	2,96	3,37837838
Thruster	10	3,81	2,62467192

Table 4 shows the results of the optimal velocity comparison between the two MHD drive configurations. The data used are the highest velocity results obtained from each configuration at the highest voltage variation. This comparison aims to evaluate the maximum performance achievable by each configuration type.

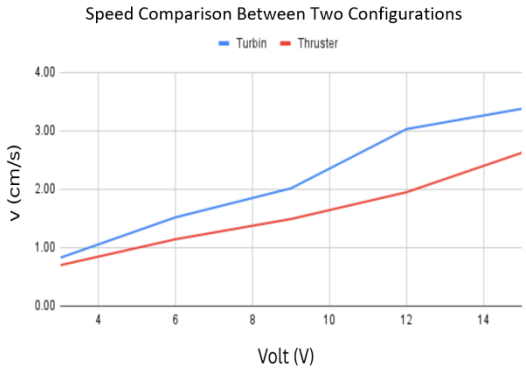

Figure 12. Graph of velocity comparison between two MHD configurations

Based on Figure 12, it can be concluded that the turbine-type configuration produces a greater optimal velocity compared to the thruster-type. This shows that under maximum voltage conditions, the turbine configuration is capable of generating stronger thrust in the seawater medium. Thus, it can be stated that the turbine configuration has better performance in generating optimal hydrodynamic velocity compared to the thruster configuration. This result also reinforces the general conclusion that electrical voltage variation affects flow velocity and that differences in MHD drive configuration affect system performance.

CONCLUSION

The test results show that the turbine-type MHD drive configuration produces greater velocity compared to the thruster-type at every voltage variation. This indicates that the turbine-type configuration is more effective in generating hydrodynamic thrust. Furthermore, the difference in configuration also affects the magnitude of the Lorentz force acting on the fluid, thus influencing the resulting water current velocity. Therefore, electrical voltage variation and MHD drive configuration are proven to affect system performance. From a broader perspective, these findings advance the scientific basis for MHD propulsion as a candidate technology for energy-efficient, noise-free marine transportation—particularly relevant for shallow-water autonomous underwater vehicles (AUVs), harbor patrol craft, and environmentally sensitive coastal applications where conventional propeller noise and cavitation are undesirable. As Indonesia pursues decarbonization of its maritime sector in alignment with IMO 2050 GHG reduction targets, MHD technology represents a long-term research investment with strategic energy policy implications. Future research could use a wider range of voltage variations and magnets with stronger magnetic fields to obtain optimal performance. Additionally, measuring electric current and using more precise measuring instruments are recommended so that the data obtained is more accurate. Subsequent research could optimize the device dimensions to produce a smaller configuration to minimize the device's mass.

ACKNOWLEDGEMENT

We would like to express our sincere gratitude to all those who have supported and contributed to the completion of this research. Special thanks to the Physics Laboratory of Kolese Kanisius, Jakarta, for providing the necessary resources and equipment. We also acknowledge the invaluable input from our research team members, particularly in the design and implementation of the MHD drive prototypes. Our deepest appreciation goes to the funding institutions and all individuals who have offered their assistance throughout this study.

AUTHOR CONTRIBUTION STATEMENT

Philipus Darwin Anwar contributed to the conceptualization of the study, the methodology, data collection, and analysis, as well as writing the original draft. Aaron Bentlee Chow was responsible for the research design, data collection, analysis, and reviewing and editing the manuscript. Erasmus Alvaro Wirosasmita provided supervision, validation, and methodology guidance, and contributed to writing the manuscript's review and editing. Agus Jarwanto participated in data collection, analysis, and reviewing and editing the manuscript. Carolina Widya Maryana contributed to the literature review, data analysis, and also assisted in reviewing and editing the manuscript.

REFERENCES

Aaron, H. M. S. (2021). Efficiency of Electric to Kinetic Energy Conversion of an Electrohydrodynamic Thruster in a Moving Bulk-Fluid. *2021 IEEE 2nd KhPI Week on Advanced Technology (KhPIWeek)*, 168–171.

Cébron, D., Viroulet, S., Vidal, J., Masson, J.-P., & Viroulet, P. (2017). Experimental and theoretical study of magnetohydrodynamic ship models. *PloS One*, *12*(6), e0178599.

Foukrach, M., Bouzit, M., Ameur, H., & Kamla, Y. (2020). Effect of agitator's types on the hydrodynamic flow in an agitated tank. *Chinese Journal of Mechanical Engineering*, *33*(1), 37. https://doi.org/10.1186/s10033-020-00454-2

Hadiningrat, K. P. S. S., Wiradanti, B., & Umar, Y. F. (2024). Transformation of Indonesian sea transportation and maritime logistics to realize the vision of Golden Indonesia 2045. *JIPOWER: Journal of Intellectual Power*, *1*(1), 89–107.

Hardianto, T., & Hadi, W. (2020). Analisis Pengaruh Lebar Celah dan Jarak Antar Magnet Terhadap Daya dan Jarak Tempuh Kapal pada MHD Channel Tipe Hall. *DIELEKTRIKA*, *7*(2), 118–124.

Javanmardi, M. H., Rahide, A., & Rouzegar, J. (2025). Magnetic Force Calculation Using Lorentz Force and Energy Conservation in Electrical Machines. *Electromechanical Energy Conversion Systems*, *4*(2), 8–34.

Lee, G. (2021). *Optimization of Lithium Charge Stripper through MHD Circulator Development*. Ulsan National Institute of Science and Technology (UNIST).

Lu, X., Li, Y., & Chen, Z. (2022). Temperature field analysis and cooling structure design of ironless permanent magnet synchronous linear motor. *Recent Advances in Electrical & Electronic Engineering (Formerly Recent Patents on Electrical & Electronic Engineering)*, *15*(1), 24–30.

Luca, R. D. (2009). Lorentz force on sodium and chlorine ions in a salt. *European Journal of Physics*, 459–466.

Mohsin, M., Abbas, Q., Zhang, J., Ikram, M., & Iqbal, N. (2019). Integrated effect of energy consumption, economic development, and population growth on CO2 based environmental degradation: a case of transport sector. *Environmental Science and Pollution Research*, *26*(32), 32824–32835.

Nago, V. G., dos Santos, I. F. S., Gbedjinou, M. J., Mensah, J. H. R., Tiago Filho, G. L., Camacho, R. G. R., & Barros, R. M. (2022). A literature review on wake dissipation length of hydrokinetic turbines as a guide for turbine array configuration. *Ocean Engineering*, *259*, 111863.

Overduin, J., Polyak, V., Rutah, A., Sebastian, T., Selway, J., & Zile, D. (2017). The Hunt for Red October II: A magnetohydrodynamic boat demonstration for introductory physics. *The Physics Teacher*, *55*(8), 460–466. https://doi.org/10.1119/1.5008337

Pawlowicz, R. (2019). *Electrical properties of sea water: theory and applications*.

Rochwulaningsih, Y., Sulistiyono, S. T., Masruroh, N. N., & Maulany, N. N. (2019). Marine policy basis of Indonesia as a maritime state: The importance of integrated economy. *Marine Policy*, *108*, 103602.

Rosmawati, T. (2011). *Ekologi perairan*. Bogor: Hilliana Press.

Salah, A. R. M. (2025). *Lorentz Force Law: Force on a Charge in Electric and Magnetic Fields*.

Tong, Z., Liu, H., Ma, J., Tong, S., Zhou, Y., Chen, Q., & Li, Y. (2020). Investigating the performance of a super high-head Francis turbine under variable discharge conditions using numerical and experimental approach. *Energies*, *13*(15), 3868.

Yusvika, M., Sutaji, A., Prabowo, A. R., Imaduddin, F., & Hadi, S. (2021). Prediction of the Hydrodynamic Performance of an Elliptical Blade Savonius Turbine using Computational Fluid Dynamics. *IOP Conference Series: Materials Science and Engineering*, *1096*(1), 12050.

Zhang, Y., Najafi, M. J., Beni, M. H., Davar, A., Toghraie, D., Shafiee, B. M., Jam, J. E., & Hekmatifar, M. (2022). The effects of geometric shapes at different assembly gaps to achieve the optimal hydrodynamic conditions. *Renewable Energy*, *184*, 452–459.

Zhou, D., Tang, J., Liu, Q., Wei, L., & Yu, D. (2021). Effects of magnetic field configuration on ionic wind characteristics. *IEEE Transactions on Plasma Science*, *49*(4), 1448–1453. https://doi.org/10.1109/TPS.2021.3064860